

# Topology Optimization Design of Impellers Based on Selective Laser Melting Process

Senpeng Fang \*, Weihao Chen, Dan Huang, Ruiwen Chen, Fuqiang Huang

AVIC Chengdu Aircraft Industry (Group) Co., Ltd., Chengdu, Sichuan, 610091, China

\* Corresponding author: Senpeng Fang

**Abstract:** Aiming at the core contradiction between structural strength and material weight reduction in the lightweight design of impellers, this paper proposes a topology optimization method considering support-free forming and blade geometric shape retention based on selective laser melting (SLM) additive manufacturing technology. The variable density method is adopted for topology optimization design, and hollow structures and lattice filling strategies are integrated to optimize the internal material distribution of impellers. SLM process constraints are introduced in the optimization process to ensure that components can be formed without additional support structures. Static mechanical performance verification of the optimized model is conducted via finite element analysis. The results show that the overall weight of the optimized model is reduced by 36% while satisfying the requirements of impeller overall dimensions and mechanical properties, which effectively balances lightweight demand, structural strength and forming process adaptability.

**Keywords:** Additive Manufacturing; Finite Element Analysis; Topology Optimization; Equivalent Stress.

## 1. Introduction

Centrifugal impellers are widely used in components such as micro gas turbines and centrifugal pumps due to their high single-stage pressure ratio and small axial size. However, the self-weight of the impeller exerts a significant impact on the overall energy consumption, response speed, and operating efficiency of the equipment. Therefore, achieving lightweight design under the premise of satisfying mechanical constraints such as strength and stiffness is the core objective of impeller structural design, which possesses important engineering application value. Against this background, topology optimization and additive manufacturing technologies, as advanced structural design and manufacturing methods respectively, have gradually attracted extensive attention.

As an effective method to enhance structural performance, topology optimization plays a vital role in realizing lightweight design, high strength and superior comprehensive performance[1]. Centering on material distribution, it autonomously searches for optimal structural configurations and component dimensions via specific algorithms under prescribed load and constraint conditions. On the premise of guaranteeing sufficient structural strength and stiffness, topology optimization can rationally arrange materials for complex structures of various specifications in accordance with practical demands and constraint limits, so as to achieve remarkable lightweight effects[2-6]. Although topology optimization enables the exploration of optimal spatial material distribution and provides great design freedom, the resulting configurations are usually highly complex and difficult to process by conventional methods, which greatly restricts its practical engineering application[7].

Metal additive manufacturing technologies represented by selective laser melting (SLM) have achieved rapid development and extensive application owing to their superior capability of free-form fabrication of intricate structures. Compared with traditional manufacturing processes such as cutting and casting, SLM eliminates the limitations of tooling, cutters and demolding constraints, and

can directly fabricate dense complex metal components with excellent mechanical properties, featuring high forming accuracy and strong structural adaptability. With its excellent compatibility with complex configurations, SLM technology realizes the deep integration of innovative configuration design based on topology optimization and free manufacturing superiority for complex structures, which effectively improves the manufacturability of topology-optimized intricate structures. For instance, Wei Wenbo[8] reconstructed the pedal bracket model by combining topology optimization with SLM technology, achieving a weight reduction of 57.1% compared with traditional structures and greatly shortening the product development cycle. However, SLM still has inherent process limitations. Specifically, there exists a critical overhang angle ranging from 40° to 50° for the downward-facing surfaces of printed parts[9]. Additional support structures are indispensable for planes with overhang angles smaller than this threshold to prevent structural collapse and warping deformation during the printing process.

With high forming freedom and material utilization rate, SLM provides a novel technical route for impeller structural optimization. Meanwhile, its inherent process characteristics including thermal stress accumulation and dependence on support structures impose stricter design requirements on topology optimization. Most existing studies mainly focus on independent topology optimization algorithms or partial structural improvement, while few systematically integrate additive manufacturing process constraints with multi-scale structural design strategies.

In view of the above research deficiencies, this paper adopts topology optimization methods and strictly complies with the process feasibility criteria of SLM. Under the constraints of external profile retention and mechanical performance requirements, the structural optimization design of a typical turbine impeller is carried out. A lightweight skeleton structure with multi-cavity characteristics for impellers is established, and the mechanical performances of the optimized model are further verified.

## 2. Structural Lightweight Design

### 2.1. Constraint Conditions and Optimization Objectives

Taking a typical centrifugal impeller as the research object for optimization analysis, the impeller is made of TC4 titanium alloy with a density of  $4440 \text{ kg/m}^3$ , elastic modulus of  $114 \text{ GPa}$ , Poisson's ratio of  $0.33$ , yield strength of  $997 \text{ MPa}$  and tensile strength of  $1027 \text{ MPa}$ . The rated operating speed of the impeller is  $58000 \text{ r/min}$  at room temperature. The lightweight-designed impeller is required to maintain its aerodynamic profile, and meet the strength criterion that its burst speed at room temperature shall not be lower than  $71000 \text{ r/min}$ .

### 2.2. Model Preprocessing

To guarantee the aerodynamic profile and assembly connection performance of blades, the internal domain of the impeller main body is designated as the optimization region. As shown in Fig.1, the internal design domain of the impeller main body is segmented, and the wall thickness of the reserved outer structure is controlled at approximately  $3 \text{ mm}$ . In addition, fillet features on the impeller are removed to simplify geometric details for subsequent numerical simulation. The whole impeller model is adopted for simulation and optimization calculation to faithfully reproduce its actual operating working conditions.

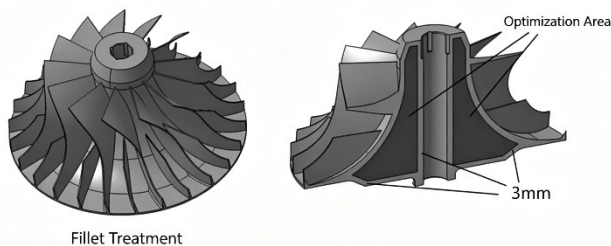


Figure 1. Impeller Model Processing

### 2.3. Optimization Design Method

This paper adopts a topology optimization-based lightweight design strategy to maximize the weight reduction of the integral centrifugal impeller while satisfying strength and stiffness requirements. Taking advantage of topology optimization in force transmission path identification, redundant materials are removed to construct a lightweight impeller structure with multiple complex cavities, fully considering the process characteristics of Selective Laser Melting (SLM).

Topology optimization is used to identify the main force transmission paths in the impeller body structure, remove redundant materials, and form an initial lightweight configuration. The topology optimization method based on the variable density method is adopted in this study, with specific settings as follows: Design variables: The internal areas of the impeller hub and backplate are defined as the design domain, and the relative density of each element is taken as the design variable. Objective function: Maximize the overall structural stiffness, i.e., maximize the reciprocal of structural compliance. Constraints: The volume fraction constraint is set to  $30\%$  of the initial volume. Manufacturing constraints: Minimum member size constraint ( $\geq 4 \text{ mm}$ ) and maximum member size constraint are introduced to ensure manufacturing feasibility and avoid unprintable fine features. A cyclic circumferential symmetric manufacturing constraint

is defined based on the impeller structural characteristics.

### 2.4. Optimization Design Flow

The lightweight design of the impeller mainly consists of three steps:

Original impeller analysis and model processing: Establish the original model according to the typical characteristics of the impeller, determine the design area, and process model details.

Impeller topology optimization analysis: Perform topology optimization analysis of the processed model with the objective of minimizing strain energy, conduct topology optimization calculations for multiple schemes, and obtain the force transmission path distribution of the impeller.

Impeller lightweight configuration design and analysis: Construct the geometric model of the optimized impeller structure based on multiple topology optimization results, carry out finite element analysis of the optimized structure under given working conditions, analyze the stress, deformation and mass of the optimized structure, compare with the original structure, and verify the feasibility of the optimized structure.

### 2.5. Design Results

A finite element model is established for the model in Figure 1, and tetrahedral mesh is adopted with a mesh size of  $2 \text{ mm}$ . The meshed model is shown in Figure 2, with  $19576$  elements and  $19744$  nodes. The material is set as TC4 titanium alloy with the parameters given above. According to the given boundary conditions, the axial displacement of the front mating surface of the integral centrifugal impeller and the circumferential torsional displacement at the impeller-shaft joint are constrained, and a rotational speed of  $58000 \text{ r/min}$  is applied.

After defining the impeller finite element model, topology optimization settings are performed. The elements in the blue region of Figure 2 are defined as the topology optimization design area, and the rest are non-design areas. The optimization objective is defined as minimizing strain energy, the optimization variable as element relative density, and the optimization constraint as volume fraction of  $0.2$ . Due to the cyclic circumferential symmetry of the impeller, cyclic circumferential symmetry constraints are applied with different parameters for the number of circumferential symmetry constraints in multiple calculations. The minimum member size is set to  $4 \text{ mm}$  to avoid excessively small force transmission frameworks.

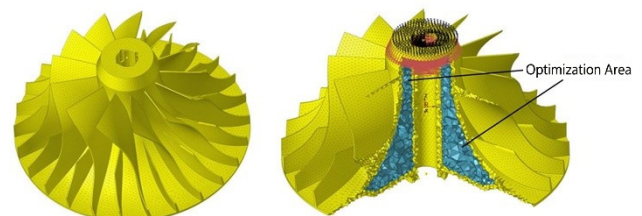


Figure 2. Finite Element Model for Impeller Topology Optimization

After calculation, the force transmission framework distribution of the impeller shown in Figure 3 is obtained. Comprehensive analysis of multiple results shows that the design area of the impeller mainly retains the transverse material in the middle and the vertical material at the lower left. Therefore, the lightweight impeller model is

reconstructed based on the analysis results. Considering that the internal support of the impeller cannot be removed, the overhang angle of the internal framework structure is set to be greater than  $45^\circ$  to eliminate the need for supports, and the minimum thickness of the structure is set to 1.5 mm.

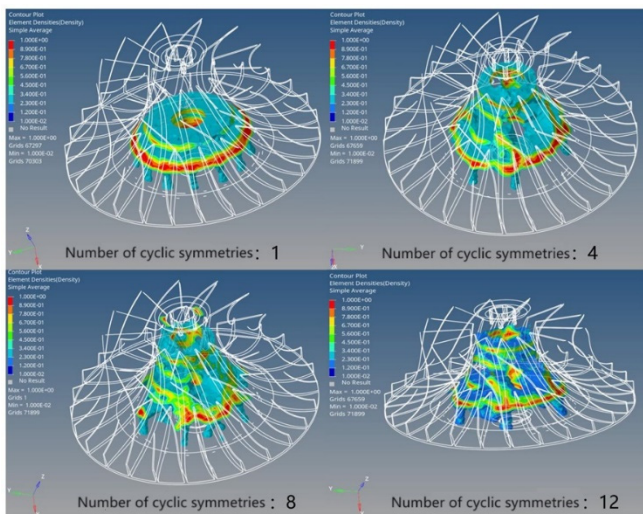


Figure 3. Impeller Topology Optimization Results

After detailed design, the lightweight impeller model is completed as shown in Figure 4. The section shows that the interior is divided into multiple cavities by multiple force transmission frameworks. Except for the outermost lower framework with a thickness of 2 mm, all other frameworks have a thickness of 1.5 mm. The boundary thickness between the impeller bottom surface and the internal axial surface is 4 mm, and the boundary thickness of the blade surface is greater than 4 mm. Finally, to ensure powder removal, powder leakage holes with radii of 2 mm and 1 mm are set inside the impeller to connect all cavities. Powder leakage holes with a diameter of 2 mm are designed on the back of the impeller and the hub to connect the interior and exterior, and the positions of the powder leakage holes on the backplate are appropriately thickened annularly with a boss.

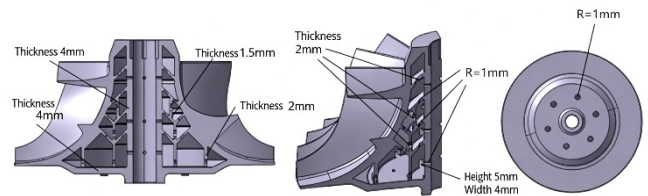


Figure 4. Reconstruction of Lightweight Impeller Model

### 3. Structural Strength Analysis

To analyze the stress and deformation of the optimized impeller structure under working speed, INTESIM software is used for mechanical analysis. After importing the impeller geometric model, tetrahedral mesh generation is performed. The material properties are shown in Table 1, and the acceleration loads are shown in Table 2. Here, X=1 represents the working speed, and X=2 represents the speed required for the optimized structure. Displacement is selected as the boundary condition, and angular velocity is selected as the load condition. The final solution yields the calculation results.

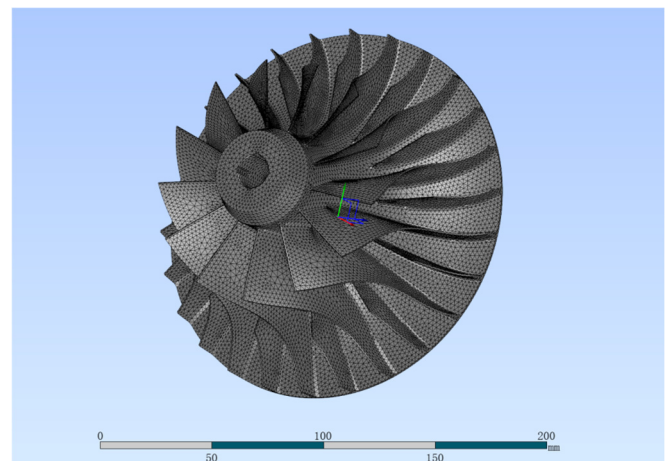


Figure 5. Impeller Mesh Model

Table 1. Key Material Parameters

Material	Temperature ( $^\circ\text{C}$ )	Elastic Modulus E (GPa)	Poisson's Ratio $\mu$	Tensile Strength $\sigma_b$ (MPa)	Yield Strength $\sigma_{0.2}$ (MPa)	Density $\rho$ ( $\text{kg}/\text{m}^3$ )
TC4	20	114	0.33	1027	997	4440

Table 2. Conversion between Rotational Speed and Angular Velocity

X	Rotational Speed (r/min)	Y Angular Velocity ( $^\circ/\text{s}$ )
1	58000	348000
2	71000	426000
3	84000	504000

#### 3.1. Strength Analysis at Working Speed

The stress contour of strength at working speed is shown in Figure 6. It can be seen that the maximum Mises stress is 798.433 MPa, which is lower than the yield stress of TC4, and is mainly located at the shaft hole at the bottom of the impeller.

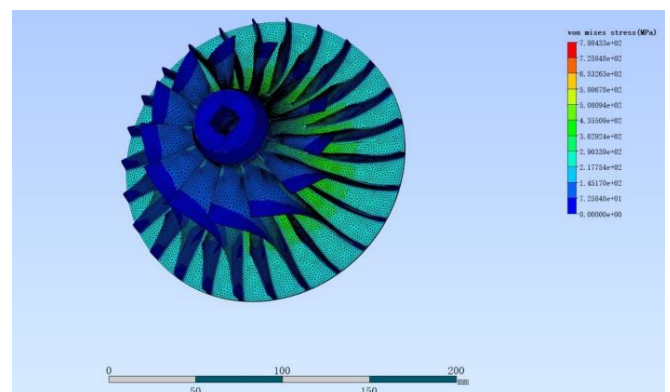


Figure 6. Maximum Mises Stress under Working Speed

#### 3.2. Strength Analysis at Burst Speed

The calculation results at the third speed, namely 84000 r/min, are exported for burst speed strength analysis. The

stress contour of burst speed strength is shown in Figure 7. It can be seen from the Mises stress contour that the maximum equivalent stress of the optimized impeller is 1023.69 MPa, mainly concentrated at the middle of the shaft hole at the bottom of the impeller. The maximum equivalent stress of the optimized impeller is close to the tensile strength of TC4 (1027 MPa). Considering simulation errors, the predicted burst speed of the optimized impeller is approximately 84000 r/min.

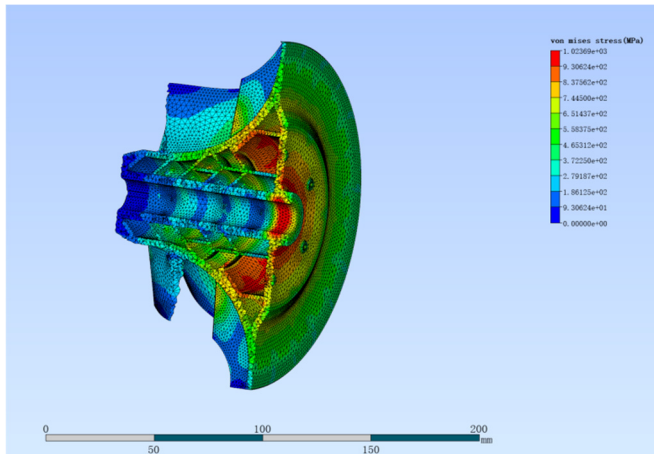


Figure 7. Maximum Mises Stress under Burst Speed

#### 4. Analysis of the Original Structure and Comparison

The original structure is analyzed for strength and compared with the optimized structure. A finite element model of the original structure is established, and tetrahedral mesh is generated with a size of 2 mm. The meshing result is shown in Figure 8, with 180520 mesh elements. The material is set as TC4 titanium alloy with the given parameters. According to the given boundary conditions, the axial displacement of the front mating surface of the integral centrifugal impeller and the circumferential torsional displacement at the impeller-shaft joint are constrained. The rotational speed of 58000 r/min is converted to an angular velocity of 348000 °/s.

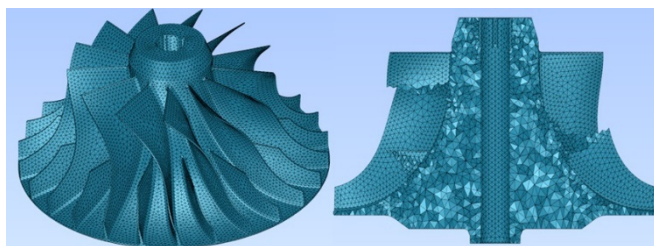


Figure 8. Mesh of Original Structure

The strength calculation result contour of the original structure model is shown in Figure 9. The maximum stress is 462.4 MPa. The internal stress distribution of the centrifugal impeller is uneven, with high-stress regions concentrated near the shaft hole. In the radial direction of the centrifugal impeller, the stress gradually decreases from the shaft hole outward, and the area of low-stress regions increases.

By comparing the finite element calculation results before and after impeller structure optimization (Figure 6 and Figure 9), it can be seen that the stress concentration regions of the optimized impeller are dispersed and no longer concentrated near the shaft hole. The weight of the optimized impeller is

reduced from 1.848 kg to 1.176 kg, with a total reduction of 36%, indicating a significant lightweight effect of the impeller structure topology optimization.

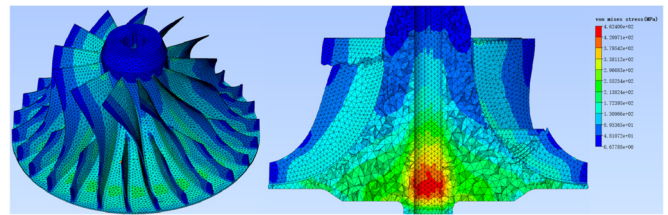


Figure 9. Stress Contour of Original Structure

#### 5. Process Feasibility Analysis

There are no surfaces  $\leq 45^\circ$  in the internal structure of the part (Figure 10), so the interior of the part can be formed independently without adding supports. In addition, the blade structure of the part is reasonably designed and can be self-formed. With optimized surface parameters, the surface roughness can be controlled to  $\leq Ra6.3$ .



Figure 10. Section of Optimized Impeller

#### 6. Conclusion

This paper conducts research on structural lightweight design, strength analysis, and process feasibility based on selective laser melting. The variable density method is used for topology optimization to identify the main force transmission paths of the impeller, and geometric reconstruction for additive manufacturing is completed based on the optimization results. Finally, a lightweight impeller structure with multiple cavities and internal framework support is formed.

On the premise of strictly meeting strength and stiffness requirements, the optimized impeller structure achieves a remarkable lightweight effect: the mass is reduced by 36% from 1.848 kg of the original structure to 1.176 kg; at the working speed (58000 r/min), the maximum equivalent stress is 798.433 MPa, which is lower than the yield strength of TC4 (997 MPa) and meets the service requirements; the predicted burst speed reaches 84000 r/min, indicating a high safety margin.

#### References

- [1] Yu H, Yang H B, Mao J, et al. Structural topology optimization based on SIMP variable density method and its application[J]. Engineering Plastics Application, 2024, 52(10): 91-99.
- [2] Liang K X, Zhu D C, Li F Y. A Fourier neural operator-based lightweight machine learning framework for topology

- optimization[J]. *Applied Mathematical Modelling*, 2024, 129: 714-728.
- [3] Ge W J, Zhu P G, Liu S L, et al. Exploring further multi-objective optimization for shape change of aircraft leading edge using compliant mechanisms[J]. *Journal of Northwestern Polytechnical University*, 2010, 28(2): 211-215.
- [4] Thompson D J, Feys J, Filewich M D, et al. The design and construction of a blended wing body UAV[C]//49th AIAA Aerospace Sciences Meeting Including the New Horizons Forum and Aerospace Exposition. Orlando: AIAA, 2011: 841.
- [5] Paz J, Díaz J, Romera L, et al. Size and shape optimization of aluminum tubes with GFRP honeycomb reinforcements for crashworthy aircraft structures[J]. *Composite Structures*, 2015, 133: 499-507.
- [6] Cavazzuti M, Costi D, Baldini A, et al. Automotive chassis topology optimization: A comparison between spider and coupé designs[C]//Proceedings of the World Congress on Engineering. London: IAENG, 2011.
- [7] Ko H Y, Shin K B, Jeon K W, et al. A study on the crashworthiness and rollover characteristics of low-floor bus made of sandwich composites[J]. *Journal of Mechanical Science and Technology*, 2009, 23(10): 2686-2693.
- [8] Wei W B. Research on topology optimization design of a folding scooter pedal bracket[J]. *Light Alloy Fabrication Technology*, 2023, 51(11): 57-62.
- [9] Kranz J, Herzog D, Emmelmann C. Design guidelines for laser additive manufacturing of lightweight structures in TiAl6V4[J]. *Journal of Laser Applications*, 2015, 27(S1): S14001.